Independency of Functional Connectivity States on Spatiotemporal Resolution of fMRI Data

Yuyuan Yang, Hui Shen, Zhiguo Luo, Fuquan Li, and Dewen Hu(✉)

College of Artificial Intelligence,
National University of Defense Technology, Changsha 410073, China
dwhu@nudt.edu.cn

Abstract. Functional magnetic resonance imaging (fMRI) is widely used to explore the brain because of its high temporal and spatial resolution. Resting-state fMRI data were studied by many researchers who found the existence of dynamic functional connectivity (dFC). However, it is unclear whether estimation of functional connectivity (FC) states is dependent on temporal and spatial resolution of sampling in fMRI data. In this paper, we addressed this concern by comparing the FC states with varying spatiotemporal resolution of data where different number of regions of interest (ROIs) were randomly chosen to extract the timecourses. These timecourses were then down-sampling to different temporal resolution. Finally, a sliding-window approach was used to estimate the potential FC states in resting-state dFC. The results show that the detection of brain connectivity is insensitive to the spatial and temporal resolution of sampled data in fMRI data, which provides a dimension reduction perspective for research based on fMRI data.

Keywords: Temporal and spatial resolution · Sliding window analysis · Dynamic functional connectivity · Cluster validity index · ROI index

1 Introduction

In recent years, considering the whole brain as a sophisticated network has obtained significant attentions, which is the so-called brain connectome [1]. Resting-state fMRI data were studied by many researchers who found the existence of dFC. In previous studies, when researchers wanted to effectively extract neural signals and capture the fluctuation information of neural signals and the dynamic activities of functional networks, they often faced the problems of the selection of brain templates [2, 3] and dealing with high dimensional data. At the same time, researchers were often confused with the choice of ROIs, from less than 100 up to the quantity of voxels, when selecting brain templates without a golden standard for the selection of nodes. Researchers had assessed topological attributes of whole-brain anatomical networks over a wide range of ROIs and found that simple binary decisions about network organization were unaffected by spatial scale [4].

There were two most common topological properties, scale-freeness and small-worldness [5], tested for brain networks. The topology of both anatomical and functional

F. Sun et al. (Eds.): ICCSIP 2018, CCIS 1006, pp. 370–380, 2019.
https://doi.org/10.1007/978-981-13-7986-4_33

brain networks was found to show small-world properties. These networks could be characterized highly clustered. Most researchers have used a set of brain templates chosen from the automated anatomical labeling (AAL) atlas [6] just because these brain templates have been widely used rather than the characteristic of their research object.

Which number of ROIs should the researchers employ? This problem can be considered of several practical issues. In particular, the researchers want to employ fine ROIs in order to reduce template-driven dependencies. This is a point of view to look for a better brain template. However, another possibility is that the choice of ROIs' numbers may be an intrinsic spatial property of the experiment object. Whether the estimation of resting-state FC states is influenced by the selection of ROIs, the changed spatial resolution in fMRI data. The best explanation is implicated in the intrinsic dimension of the resting-state brain states. We suppose that the intrinsic dimension of the resting-state brain states is much lower than the thousands of dimensional data. Then, when different numbers of ROIs are altered to extract the timecourses, the FC states should be similar. Different numbers of ROIs change the spatial solution of data. Furthermore, the FC states should exhibit the similar phenomenon with spatial and temporal solution changing. To verify the assumption the experiments were conducted by using different numbers of ROIs and different temporal solution timecourses to explore the effect to the brain functional connectivity under data with different temporal and spatial resolutions.

2 Datasets

2.1 HCP Dataset

Healthy subjects were selected from the public data set of the Human Connectome Project (HCP, http://www.humanconnectomeproject.org/). The data of the subjects under resting states were collected by a 3.0T nuclear magnetic resonance apparatus with the following parameters: flip angle = 52°, time repetition = 720 ms, slice number = 72, 1200 volumes were obtained.

2.2 COBRE Dataset

The COBRE (The Center for Biomedical Research Excellence http://Functional-Connectionon_1000.projects.nitrc.org/indi/retro/cobre.html) dataset is a public data set for conducting biomedical researches.

All data were scanned with a 3.0T Siemens NMR scanner with the following parameters: time repetition = 2 s, layer thickness = 3.5 mm, slice gap = 1.05 mm, matrix size = 64 × 64, FOV = 240 mm, 150 volumes were obtained. The resting state fMRI data of 50 healthy subjects were randomly selected from the healthy subjects for the experiment.

3 Methods

3.1 Data Preprocessing and Spatial Sampling

The preprocessing software package was SPM8 (Wellcome Department of Imaging Neuroscience, University College London, UK, http://www.fil.ion.ucl.ac.uk/spm). (1) For each subject, the first several frames of scanned images were removed to reduce the magnetic saturation; (2) Slice timing; (3) Head motion correction; (4) Processed fMRI images for each frame based on standard templates to extract the grey-matter signals and, which was called as spatial normalization. This procedure changed the spatial solution of original data. (5) Spatial smoothing using Gaussian filtering with FWHM = 6 mm; (6) Filtering processing with frequency of 0.01 Hz–0.08 Hz (7) Regression of the whole brain's global signal (GS), head motion, white matter (WM), cerebrospinal fluid (GSF) to reduce noises.

Through the above preprocessing steps, then the ROI generated with the brain parcellation algorithm [4] could be used to extract ROI-based timecourse from 4-D fMRI data. The obtained blood oxygenation level dependent (BOLD) signal timecourses which could be used to calculate the functional connectivity were obtained [7]. When the time signal was extracted from the preprocessed data, the spatial resolution of the timecourses was changed by selecting different numbers of ROIs, and statistical methods were used to calculate the clustering validity index [8]. Exploring the relationship between the different numbers of ROIs and the number of clusters could avoid the problem of comparing FC state matrices with different dimensions. In the statistics, the evaluation criterion of FC states is the cluster validity index under different ROIs.

3.2 Data Temporal Sampling

This method was opted to use when exploring the changing temporal solution's effect on the FC states. Before carrying out the sliding window analysis, the original timecourses (TR = 0.72 s) could be down-sampled, and the timecourses with the temporal resolution of 2TR (1.44 s), 4TR (2.88 s), and 8TR (5.76 s) were obtained. Under-sampling the timecourses under resting conditions, thus changing the data temporal resolution, sliding window analysis processing is performed for the same timecourses with different temporal resolutions, and the brain connectivity state matrix is obtained by spectral clustering. The similarity of brain connectivity matrices are measured by Pearson correlation.

3.3 Sliding Window Analysis

The input data for the sliding window analysis is a set of timecourses representing the activity signals in the brain region. In the simplest case, select the window length of the time window that is parameterized with W, and using the window size (from t = 1 to t = W) [2] to calculate the connection correlation for each pair of timecourses. The Pearson correlation coefficient is used as a statistical measurement method. Then, the time window is backwards, sliding step = T, and repeating the same step with the window size [1 + T, W + T] [3]. The sliding calculation process iterates through the window to the end portion containing the entire timecourses, and finally obtains the

connectivity. There are N elements of different regions, and the matrix size of the data information recorded in each window is N × (N − 1)/2. At the same time, considering all the matrices together, a set of dFC is obtained [9–11].

Bivariate correlation is the most direct measure of evaluating functional connections in the sliding window approach [12]. In this experiment, the Pearson correlation coefficient commonly which used in the bivariate correlation method can be used to calculate the dynamic functional connectivity correlation of each pair brain regions [13]. The timecourses is set as a function of the time t which is an independent variable, where in the seed region is represented by s(t), t = 1, 2, …, n. The region of interest is r(t), t = 1, 2, …, n means, $\bar{s}$ is the mean of s(t), $\bar{r}$ is the mean of r(t). The correlation formula of the two regions is:

$$c = \frac{\sum_{t=1}^{n} (s(t) - \bar{s})(r(t) - \bar{r})}{\sqrt{\sum_{t=1}^{n} (s(t) - \bar{s})^2 \times \sum_{t=1}^{n} (r(t) - \bar{r})^2}} \tag{1}$$

In the subsequent statistical analysis, for the convenience of statistics, the Fisher value is replaced by the Fisher value by the Fisher z-transform, and the transformation formula is as follows:

$$z = \frac{1}{2}\log\left(\frac{1+c}{1-c}\right) \tag{2}$$

This transformation causes a large change in the z value in the vicinity of c = −1 and c = 1, thereby enhancing the normal distribution characteristic of the correlation coefficient c.

In the experiment, the correlation between the timecourses of all regions is calculated, that is, all brain regions are sequentially set as seed regions.

3.4 Spectral Clustering

Spectral clustering is based on graph theory, and the essence is to transform clustering into graph segmentation problem.

Input: sample points $S = \{s_1, \ldots, s_n\}$, number of clusters k example
Output: label vector
Algorithm flow:
To measure the similarity of sample points, construct the adjacency matrix $A \in R^{n*n}$, where $A_{ii} = 0$;

Constructing matrix

$$D_{ii} = \sum_{j=1}^{n} A_{ij} \tag{3}$$

Laplacian matrix

$$L = D^{-\frac{1}{2}} A D^{\frac{1}{2}} \tag{4}$$

Calculate the first k largest eigenvectors $x_1, x_2, \cdots, x_k$ in L, and then rank the eigenvectors into a matrix in the order of the columns;

$$X = [x_1, x_2, \cdots, x_k] \in R^{n \times k} \tag{5}$$

Each row of the matrix X is unitized and converted into a matrix Y, where

$$Y_{ij} = X_{ij} / (\sum\nolimits_j X_{ij}^2)^{1/2} \tag{6}$$

A row of Y is a sample point in the k-dimensional Euclidean space, and the k-means algorithm is used to cluster the n sample points into k-class;

Finally, the sample point s_j is assigned to the j class if and only if the i row of Y is assigned to the j class.

4 Experiments and Results

4.1 Temporal Solution Experiments

The timecourses of fMRI images were obtained with the brain template of 160, and the original timecourses were with the temporal resolution of time repetition = 0.72 s.

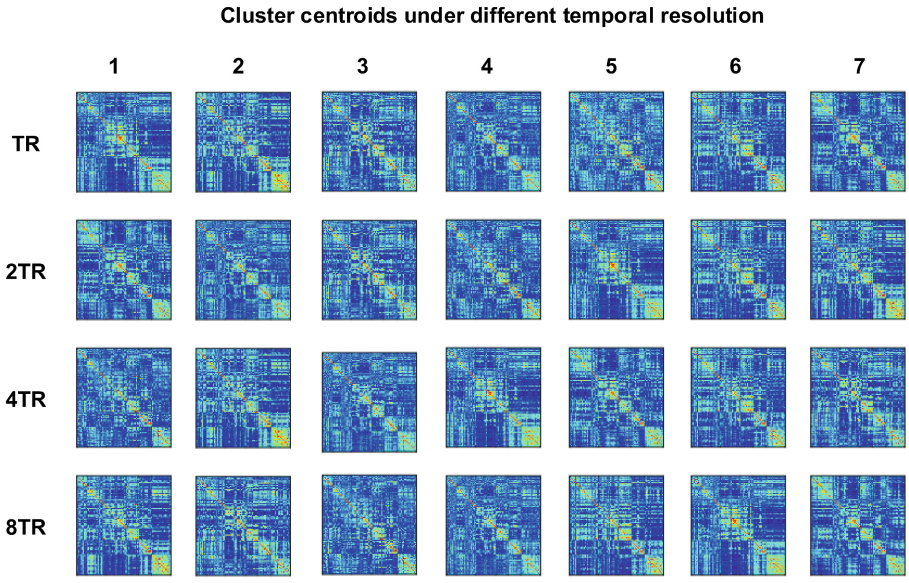

Fig. 1. The resting state fMRI data's brain connectivity under different temporal solution

The timecourses were down-sampled with the temporal resolution of 2TR, 4TR, and 8TR were obtained. When constructing the dynamic function connection matrix, the window parameters with the window size of 40 s and the sliding step length of 10 s were used to calculate and get results. During the research on resting state fMRI data conducted, a significant phenomenon appears. In the Fig. 1 (A): These cluster centroids graphs show the brain functional dynamic connectivity states. Seven clustering centers are obtained under different temporal solution when the solution of original brain timecourses' reduction varying from 1TR, 2TR, 4TR to 8TR.

Even the original data have different temporal solution. After sliding window correlation analysis and spectral clustering, their brain connectivity states do not change significantly.

For example, in the Table 1: Under 1TR's and 8 TR's temporal solution, the seven clustering centers have the most far similarity in the experiment. But we can see, the lowest central similarity is still above 93.30%. provides when the solution of original brain timecourses' reduction varying from 1TR, 2TR, 4TR to 8TR.

Table 1. The Pearson correlation between the clustering centroids under 1TR and 8TR resolution

	1	2	3	4	5	6	7
1	**98.83%**	70.85%	70.46%	71.65%	64.32%	71.39%	63.53%
2	71.55%	**95.91%**	62.67%	69.57%	63.62%	73.75%	64.51%
3	68.86%	63.51%	**98.88%**	70.76%	62.26%	66.11%	66.95%
4	72.55%	70.97%	70.53%	**98.57%**	63.92%	70.16%	71.66%
5	58.31%	66.45%	55.23%	63.71%	**96.99%**	64.37%	63.61%
6	67.21%	77.88%	63.95%	69.76%	67.76%	**96.87%**	72.70%
7	68.79%	68.83%	66.79%	67.26%	67.13%	64.29%	**93.78%**

4.2 Spatial Resolution Experiments

This part of the experiment used data from 50 healthy subjects of COBRE. In the process of extracting timecourses, 50, 116, 160, 257, 376, 459, 808 ROIs were used, which were randomly selected from 50–800 generated ROIs [4]. The principle of the brain template in extracting signals is actually to take the average of the signals of all voxels in a single brain region defined in the brain template, and the coordinates of the signal are defined as the central position of the region.

Due to the experiment using different numbers of ROIs, while changing the spatial resolution of data sampling, also have an impact on the dimensions of the final brain connection state matrix, in this part of the study, we couldn't measure the similarity of brain state by evaluating the similarity of the cluster centers' similarity.

The use of clustering validity index to evaluate the change of sampling spatial resolution is enough to affect the detection of the number of FC states, and to compare the relationship between clustering validity index and cluster numbers under different spatial resolutions.

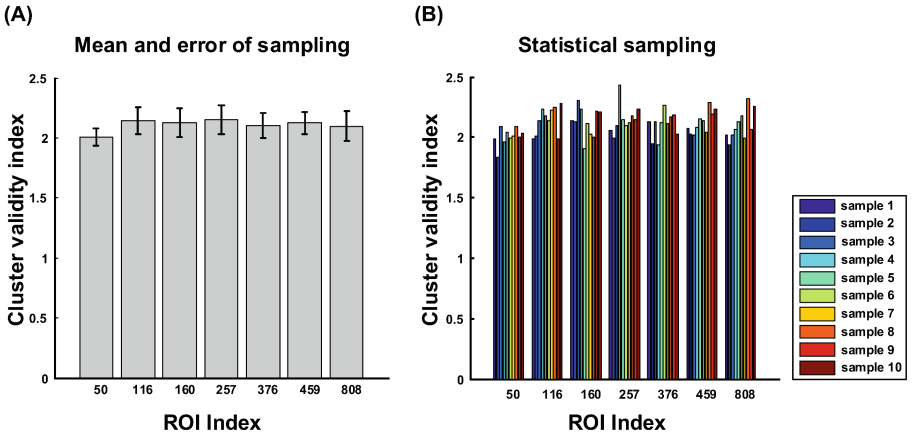

Fig. 2. The statistical analysis between the Cluster validity index and ROI index

The timecourses of 50 subjects were used to make the experimental data more general and persuasive when calculating the clustering validity index. 50 timecourses were selected each time, and 10 times were repeated to obtain ten sets of data. The ten groups of clustering validity index, the statistical analysis, are shown in the Fig. 2.

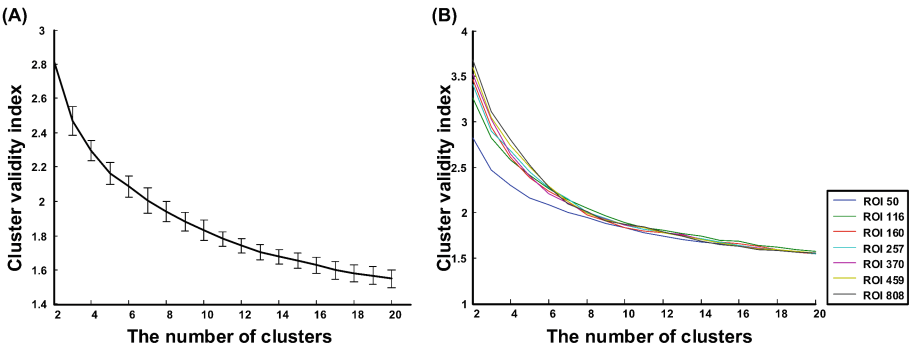

Fig. 3. The cluster validity index plotted as a function of the number of clusters. In particular, the graph (A) indicates the relation between the cluster validity index mean and standard deviation of 10 times statistical analysis and the number of clusters when ROIs are equal to 50. The graph (B) displays the relation between the cluster validity index mean and the number of clusters when ROIs are equal to 50, 116, 160, 257, 370, 459 and 808.

To get a detailed information contained in the data,we calculate the mean and standard deviation among the statistical analysis. In Fig. 4(A), the data are presented in the other style graph and cluster validity index are calculated in sampling statistics. When doing statistics, the timecourses of 50 subjects are as a sample population and 50 sets of timecourses are selected each time. Ten times were repeated to be selected to

obtain ten sets of data. We obtained data on the relationship between clustering validity index and clustering numbers in 10 groups at 7 different spatial resolutions. Let us take the 10 sets of data as a Fig. 3 with the number of 50 ROIs. In the Fig. 3(A) linear graph, with the increase of the number of clusters, the trend of clustering validity index is: As the number of clusters decreases rapidly from 2 to 5, then the changes become slower and slower, and the rate of clustering index changes greatly. The number of nearby clusters is most likely the true number of brain connections we want to detect. In the Fig. 3(B), the cluster validity index all show the similar descending speed trend under different ROIs. When the number of clusters was 2 to 5, it decreased sharply with the increase of the number of clusters: when the number of clusters was 5 to 10, the change starts slowly. What's more, the cluster validity index under different number of ROIs become quickly approaching when clusters' number varying from 5 to 10.

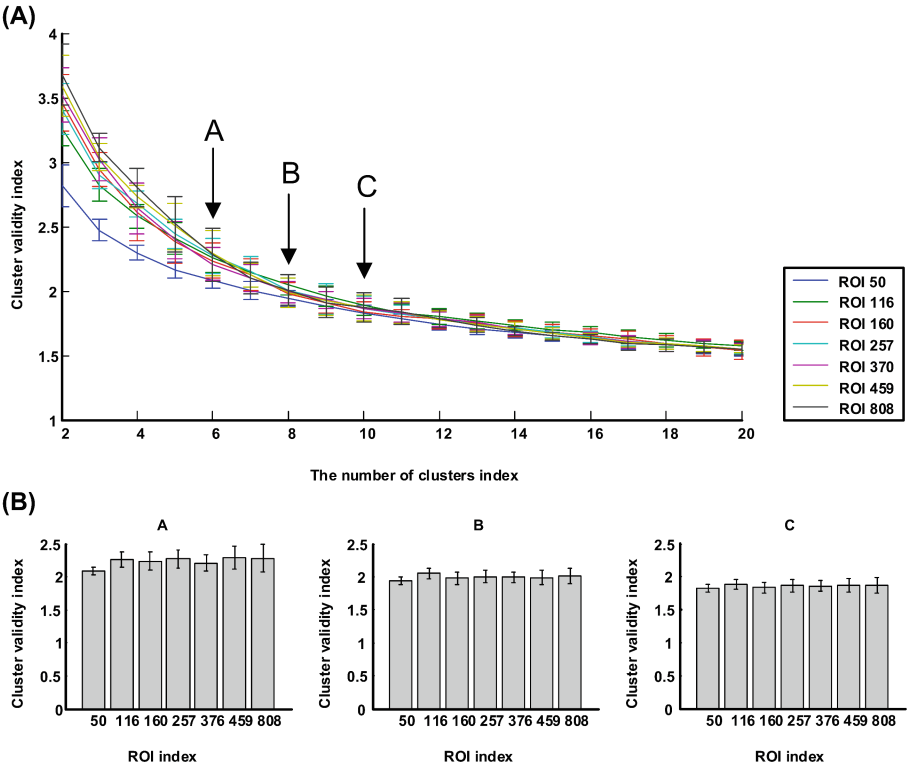

Fig. 4. The mean and standard deviation of cluster validity index under different number of clusters and different number of ROIs.

When the number of clusters is around 8, the clustering evaluation indicators are not much different. When the number of clusters is 10, the clustering index indicators calculated under different number of ROIs overlap. Mean and variance in sampling statistics under different number of ROIs are drawn. In Fig. 4(B), the slice A, B and C

are obtained under different clusters' numbers from the Fig. 4(A), and for example, the slice A is obtained when cluster number equals 6. In the Fig. 4(B) A, the bar illustrates the cluster validity index are approaching closely. In the Fig. 4(B) B, when the number of clusters index equals 8, the cluster validity index is mixed under different clusters' numbers. In Fig. 4(B) C, the cluster validity index is nearly equal to each other under different clusters' numbers.

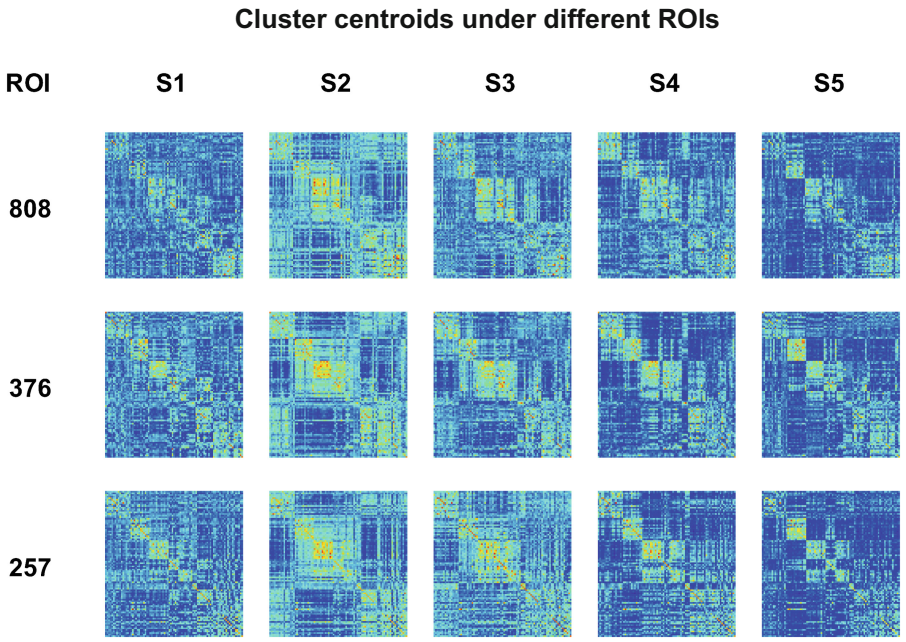

Fig. 5. The resting state fMRI data's brain connectivity under different ROIs. These cluster centroids are similar with the ROIs changing.

The Fig. 5 is an abridged general view and when ROIs are changing from 808, 376 to 257, the cluster centroids under cluster number 5 are still showing consistency. To confirm the results, quantitative analysis of these centroids is conducted. The accurate similarity among the cluster centroids are showed in the Table 2.

Table 2. The states labels' accurate consistency under 808, 376 and 257 ROIs.

	1	2	3	4	5	Ratio (%)
808	1	2	3	4	5	100
376	5	2	1	3	4	80.38
257	2	3	1	4	5	76.38

To get a more detailed information, all subjects' dynamic connectivities in correlation window are analyzed. The dynamic connectivity analysis in every subject gives a interpretation to the inconsistent of the state labels in Table 2. These inconsistency focus on the change of the subjects and the state change in every subject under cluster number 5 as shown in Fig. 6.

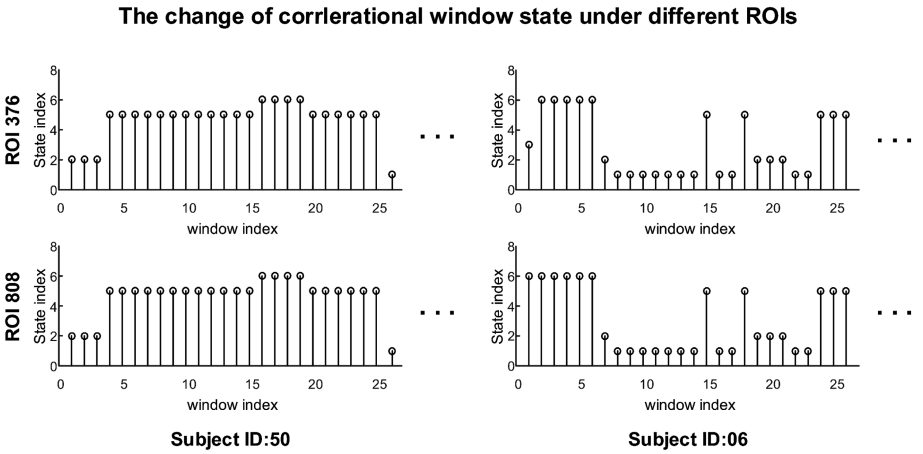

Fig. 6. When the cluster equals 7, the dynamic connectivities are shown at every sliding window under ROI 376 and ROI 808. The inconsistency of states labels at the same sliding window mainly occurs in the boundaries of the change of subjects.

5 Discussion

In order to explore the influence of the spatiotemporal resolution of data sampling on the determination of dFC, these experiments were conducted and some interesting results were obtained. When down-sampling the timecourses, the similarity of clustering center was measured by Pearson correlation. When the time resolution was increased from 0.72 s to 5.76 s, the determination of FC states had not been greatly affected. When the spatial resolution of the timecourses was changed by selecting different ROIs, the clustering validity index calculated in statistics analysis showed a similar descending speed trend with the number of clusters changing under different ROIs.

These results confirm the estimation of FC states is independent on temporal and spatial resolution of sampling in resting-state fMRI data. At the same time, it may indicate that the brain intrinsic dimension under resting-state is lower than the number of ROIs used in this paper. The results also verify some past research findings. These researches used dimensionality reduction methods to find the brain activity patterns of global and local nerve tissue [14, 15]. The manifold decoding was used to represent the features embedded in spatiotemporal brain activity. Inspired from these studies and our findings, our future work is using dimensionality reduction coding algorithms to explore the structural of dFC states under resting-state and excavating the intrinsic information hidden in the massive fMRI data.

Acknowledgement. This research was in part supported by grants from the National Science Foundation of China (61773391, 61503397 and 61420106001).

References

1. Sporns, O., Tononi, G., Kotter, R.: The human connectome: a structural description of the human brain. PLoS Comput. Biol. **1**, e42 (2005)
2. Allen, E.A., Damaraju, E., Plis, S.M., Erhardt, E.B., Eichele, T., Calhoun, V.D.: Tracking whole-brain connectivity dynamics in the resting state. Cereb. Cortex **24**, 663–676 (2014)
3. Zhang, Z.G., et al.: Adaptive window selection in estimating dynamic functional connectivity of resting-state fMRI, pp. 1–4 (2013)
4. Zalesky, A., et al.: Whole-brain anatomical networks: does the choice of nodes matter? Neuroimage **50**, 970–983 (2010)
5. Amaral, L.A.N., Scala, A., Barthélémy, M., Stanley, H.E.: Classes of small-world networks. Proc. Natl. Acad. Sci. U.S.A. **97**, 11149–11152 (2000)
6. Tzourio-Mazoyer, N., et al.: Automated anatomical labeling of activations in SPM using a macroscopic anatomical parcellation of the MNI MRI single-subject brain. Neuroimage **15**, 273–289 (2002)
7. Shen, H., et al.: Changes in functional connectivity dynamics associated with vigilance network in taxi drivers. Neuroimage **124**, 367–378 (2016)
8. Anderson, D.T., Zare, A.: Spectral unmixing cluster validity index for multiple sets of endmembers. IEEE J. Sel. Top. Appl. Earth Obs. Remote Sens. **5**, 1282–1295 (2012)
9. Elton, A., Gao, W.: Task-related modulation of functional connectivity variability and its behavioral correlations. Hum. Brain Mapp. **36**, 3260–3272 (2015)
10. Kucyi, A., Davis, K.D.: Dynamic functional connectivity of the default mode network tracks daydreaming. Neuroimage **100**, 471–480 (2014)
11. Hutchison, R.M., Morton, J.B.: Tracking the brain's functional coupling dynamics over development. J. Neurosci. Off. J. Soc. Neurosci. **35**, 6849–6859 (2015)
12. Leonardi, N., Van De Ville, D.: On spurious and real fluctuations of dynamic functional connectivity during rest. Neuroimage **104**, 430–436 (2015)
13. Hindriks, R., et al.: Can sliding-window correlations reveal dynamic functional connectivity in resting-state fMRI? Neuroimage **127**, 242–256 (2016)
14. Kuo, P.C., Chen, Y.S., Chen, L.F.: Manifold decoding for neural representations of face viewpoint and gaze direction using magnetoencephalographic data. Hum. Brain Mapp. **39**, 2191–2209 (2018)
15. Saul, L.K., Roweis, S.T.: Think globally, fit locally: unsupervised learning of low dimensional manifolds. J. Mach. Learn. Res. **4**, 119–155 (2003)